

Using a Modern Radiation Dose Model to Investigate Exposure Rates During GLE 73

Nicholas Larsen,^{a,*} Alexander Mishev^{a,b} and Ilya Usoskin^{a,b}

^a*Sodankylä Geophysical Observatory,
University of Oulu, Tähteläntie 62, Sodankylä, Finland*

^b*Space Physics and Astronomy Research Unit,
University of Oulu, Pentti Kaiteran katu 1, Oulu, Finland*
E-mail: nicholas.larsen@oulu.fi, alexander.mishev@oulu.fi,
ilya.usoskin@oulu.fi

Solar energetic particles (SEPs) are created by solar eruptions and their aftermath. These SEPs pose a significant space weather threat, as they can be accelerated to energies needed to penetrate the Earth's magnetosphere and enter the atmosphere, where they increase the radiation environment at high altitudes, specifically endangering the health of aircrew and airline passengers. Secondary particles of the SEP-induced atmospheric cascades can reach the Earth's surface where ground-based detectors, such as neutron monitors (NMs) can record them, when this occurs it is known as a ground-level enhancement (GLE). Solar cycle 25 had its first GLE on 28 October 2021, named GLE 73. This GLE was mainly detected by NMs at the Antarctic plateau (SOPO and DOMC). In recent work, GLE 73 has been analysed using a verified method and the NM data from the event to derive its spectral and anisotropic characteristics. Here, we present an application of said derived characteristics for GLE 73 by using them as inputs into a newly developed radiation dose model for GLE events. This model was applied over the entire duration of the event resulting in a comparison between the relative increases in radiation dose and NM count rate for GLE 73.

38th International Cosmic Ray Conference (ICRC2023)
26 July - 3 August, 2023
Nagoya, Japan



*Speaker

1. Introduction

The Sun is a highly volatile object made up of ionised plasma and heated by nuclear fusion in its core. One of the most dangerous byproducts of the Sun's structure is the resulting solar eruptions that can occur, which release large fluxes of particles and energy into the heliosphere [1]. Certain solar eruptions can lead to particles being accelerated up to relativistic energies, we call these particles solar energetic particles (SEPs). When SEPs are created it is known as an SEP event. These SEP events can last from several hours up to multiple days, the SEP spectra over this period can change dramatically [2].

The SEPs from solar eruptions, primarily protons and helium nuclei [3], can be directed at Earth. Depending on the energy of the SEPs they can be able to penetrate the Earth's magnetosphere and enter into the atmosphere. The energy or rigidity, rigidity is typically used as it is independent of the particle's species and refers to the ability of a magnetic field to bend the path of the said particle [4], needed by the particle to penetrate the magnetosphere depends heavily on the location it arrives at the Earth, this is known as the cut-off rigidity. Equatorial regions have higher cut-off rigidity values, ≈ 15 GV, whereas polar regions have much lower values, being ≈ 0 GV at the magnetic poles [5].

Once a high-energy particle, such as an SEP, penetrates the atmosphere it induces a complex atmospheric shower as it collides with the atmospheric constituents to produce secondary particles. The secondary particles can then reach the Earth's surface, given the incident particle had sufficient energy, where they can be detected by ground-based equipment, such as neutron monitors (NMs). When a significant increase in SEP flux is detected at the surface by several NMs it is known as a ground-level enhancement (GLE) [6]. GLEs are fairly sporadic in nature and only a few occur per solar cycle, typically during solar maximum when the Sun is most active [7].

GLEs are associated with several space weather risks, such as damaging electronics in spacecraft and enhancing the radiation environment at high altitudes, this work focuses on the latter. The mixed radiation field is enhanced by the arrival of the SEPs into the atmosphere where the particles can damage human DNA, which, depending on the dose received, can lead to radiation poisoning and cancer. Naturally, the aviation industry is interested in mitigating the danger posed by SEP events as it primarily affects aircraft crews and passengers who are at risk of higher exposures. As such, investigating the impact that GLEs have on the radiation at flight altitudes is crucial in developing nowcasting methods to help mitigate the impact future GLEs can have on human health. GLEs must be studied individually due to each one having different characteristics such as their spectra, particle flux, duration, and angular distribution [8, 9].

GLE 73 was the first GLE of solar cycle 25, which occurred on 28 October 2021. This was a relatively weak event with less than a 20% increase in the count rate detected by NMs in comparison to the galactic cosmic ray (GCR) background. This is the most recent GLE at the time of writing and the impact of this GLE on the radiation dose received at flight altitudes is investigated within this work.

2. SEP Spectrum

In order to determine the impact of a GLE on the radiation at high altitudes the SEP spectra must first be unfolded. This is done by modelling the response of the NM network during the event to determine the SEP characteristics and apparent source position. This can be done by taking advantage of the stationary nature of NMs, as each one is sensitive to different rigidities of particles and their arrival directions. This means that the NM network in conjunction with the Earth's magnetic field can be used as a giant particle spectrometer.

The spectral analysis on GLE 73 has already been conducted using methodology detailed in previous work (for more details see [10–14] and references therein). This method involves modelling the NM response using the Levenberg-Marquardt algorithm [15, 16] and optimisation methods to find reasonable solutions to ill-posed problems. The SEP rigidity spectrum is approximated by two modified power-laws, one for rigidities above 1 GV and another for rigidities equal to and below 1 GV, Eq. 2 and Eq. 1 respectively,

$$J_{\parallel}(P) = J_0 P^{-(\gamma + \delta\gamma(P-1))} \quad (1)$$

$$J_{\parallel}(P) = J_0 P^{-(\gamma + \delta\gamma \cdot P)} \quad (2)$$

where $J_{\parallel}(P)$ is the flux of particles along the axis of symmetry in $[\text{m}^{-2}\text{s}^{-1}\text{sr}^{-1}\text{GV}^{-1}]$, J_0 is the flux of particles at 1 GV, P is the rigidity in [GV], γ is the power-law exponent, and $\delta\gamma$ is the steepening.

A merit function (Eq. 3) is also used to determine the quality of the fit,

$$\mathcal{D} = \frac{\sqrt{\sum_{i=1}^m \left[\left(\frac{\Delta N_i}{N_i} \right)_{\text{mod.}} - \left(\frac{\Delta N_i}{N_i} \right)_{\text{meas.}} \right]^2}}{\sum_{i=1}^m \left(\frac{\Delta N_i}{N_i} \right)_{\text{meas.}}} \quad (3)$$

where N is the NM network response. The merit function is useful as it informs us of the strength of the GLE. Strong events have a $\mathcal{D} \leq 5\%$ and weak events have typical values ranging from $\approx 10\text{--}15\%$, for some weak events it can even rise to 20% [13].

The results of the SEP spectra analysis for GLE 73 can be seen in table 1 [10].

3. Radiation Model

The newly developed radiation model known as Oulu CRAC:DOMO (Cosmic Ray Atmospheric Cascade: Dosimetric Model) was used in this work [17]. This model has been used due to its recent verification by direct HEMERA-2 stratospheric scientific balloon measurements [18]. Once the SEP rigidity spectrum for a GLE event is obtained an effective dose can be computed using Eq. 4

$$E(h, T, \theta, \varphi) = \sum_i \int_{T_{P_{\text{cut}}}}^{\infty} \int_{\Omega} J_i(T) Y_i(T, h) d\Omega(\theta, \varphi) dT, \quad (4)$$

where $J_i(T)$ is the differential energy spectrum of the primary SEPs and Y_i is the corresponding effective dose yield function for a given altitude and energy. The yield functions used within this model were computed using extensive Monte Carlo simulations performed to model the

Table 1: Spectral and angular characteristics of SEPs during GLE 73 on 28 October 2021 [10]. The columns correspond to integration interval (1), particle flux (2), spectrum slope (3), steepening of the spectrum (4), width of the angular distribution (5), anisotropy axis latitude Ψ (6), anisotropy axis longitude Λ (7), merit function \mathcal{D} (8), and normalised to degrees of freedom χ_r^2 (9).

Integration interval UT	J_0 [$\text{m}^{-2}\text{s}^{-1}\text{sr}^{-1}\text{GV}^{-1}$]	γ	$\delta\gamma$	σ^2 [rad^2]	Ψ [degrees]	Λ [degrees]	\mathcal{D} [%]	χ_r^2
15:55–16:00	7.5E4	4.1	1.3	2.7	-10.0	-124.0	22	1.3
16:00–16:05	7.7E4	4.2	1.2	2.8	-12.0	-127.0	21	1.3
16:05–16:10	7.89E4	4.2	1.1	2.8	-13.0	-128.0	23	1.3
16:10–16:15	8.1E4	4.3	0.9	2.9	-14.0	-130.0	19	1.2
16:15–16:20	8.2E4	4.3	0.8	2.9	-15.0	-131.0	14	1.2
16:20–16:25	8.75E4	4.4	0.8	3.0	-21.0	-132.0	12	1.15
16:25–16:30	9.1E4	4.4	0.8	3.1	-30.0	-132.0	11	1.1
16:30–16:35	9.4E4	4.5	0.8	3.1	-34.0	-135.0	7.0	1.0
16:35–16:40	9.48E4	4.7	0.75	3.2	-31.0	-137.0	9.0	0.99
16:40–16:45	9.58E4	4.8	0.7	3.3	-35.0	-140.0	8.0	0.95
16:45–16:50	9.67E4	4.9	0.6	3.5	-38.0	-140.0	12	1.1
16:50–16:55	9.85E4	5.1	0.5	3.7	-37.0	-142.0	11	1.1
16:55–17:00	1.01E5	5.3	0.5	3.9	-40.0	-145.0	12	1.15
17:00–17:05	1.038E5	5.5	0.4	4.2	-50.0	-148.0	10	1.1
17:05–17:10	1.05E5	5.5	0.4	4.2	-50.0	-148.0	10	1.1
17:10–17:15	1.06E5	5.5	0.4	4.2	-48.0	-147.0	12	1.2
17:15–17:20	1.08E5	5.6	0.37	4.2	-50.0	-148.0	11	1.1
17:20–17:25	1.112E5	5.7	0.36	4.3	-52.0	-148.0	9.0	1.05
17:25–17:30	1.134E5	5.75	0.35	4.4	-54.0	-150.0	10	1.1
17:30–17:35	1.148E5	5.8	0.35	4.5	-57.0	-151.0	11	1.1
17:35–17:40	1.152E5	5.9	0.35	4.7	-61.0	-151.0	12	1.15
17:40–17:45	1.171E5	6.0	0.3	4.9	-54.0	-152.0	11	1.1
17:45–17:50	1.192E5	6.1	0.3	5.1	-55.0	-153.0	12	1.1
17:50–17:55	1.21E5	6.25	0.3	5.3	-52.0	-151.0	10	1.1
17:55–18:00	1.241E5	6.3	0.3	5.3	-57.0	-154.0	13	1.2
18:00–18:05	1.25E5	6.3	0.3	5.3	-58.0	-155.0	11	1.1
18:05–18:10	1.27E5	6.4	0.25	5.5	-54.0	-157.0	12	1.1
18:10–18:15	1.29E5	6.5	0.2	5.7	-52.0	-157.0	11	1.1
18:15–18:20	1.314E5	6.5	0.2	5.9	-55.0	-158.0	13	1.15
18:20–18:25	1.25E5	6.6	0.2	6.1	-50.0	-160.0	10	1.1
18:25–18:30	1.21E5	6.7	0.2	6.3	-45.0	-161.0	9.0	1.05
18:30–18:35	1.15E5	6.9	0.2	6.5	-42.0	-162.0	12	1.2
18:35–18:40	1.11E5	7.0	0.15	6.7	-37.0	-162.0	10	1.1
18:40–18:45	1.074E5	7.0	0.15	6.9	-33.0	-165.0	11	1.15
18:45–18:50	1.032E5	7.1	0.15	7.3	-31.0	-166.0	12	1.2
18:50–18:55	1.01E5	7.1	0.1	7.5	-27.0	-167.0	13	1.2
18:55–19:00	1.0E5	7.2	0.1	7.7	-24.0	-168.0	12	1.2
19:00–19:15	9.5E4	7.3	0.0	7.7	-20.0	-168.0	11	1.2
19:15–19:30	9.3E4	7.5	0.0	7.9	-24.0	-171.0	10	1.2
19:30–19:45	9.1E4	7.6	0.0	8.1	-27.0	-173.0	12	1.25
19:45–20:00	8.5E4	7.7	0.0	8.3	-18.0	-175.0	13	1.3

POS (ICRC2023) 1261

atmospheric cascades induced by protons and helium nuclei, which comprise the majority of SEPs [19]. Integrating with respect to the kinetic energy (T) up to infinity, starting at the energy corresponding to the cut-off rigidity ($T_{P_{cut}}$) of the local area leads to the effective dose for that region.

4. Results

The radiation model was applied to a global map of the cut-off rigidity for GLE 73 computed by a new tool designed for magnetospheric trajectory computations, called "Oulu - Open source geomageToSphere prOpagation tool" (OTSO) [20]. The total exposure during GLE 73 was computed for an altitude of FL350 (35kft), the typical aviation altitude for flights. The result of this is shown in Fig. 1. Fig. 1 shows that the greatest exposure was seen in the polar regions, due to the lower magnetic shielding, with the exposure reaching $46.0\mu\text{Sv}$ in these regions. The exposure in equatorial regions was much smaller, with the lowest exposure of $7.1\mu\text{Sv}$ being seen in southern Asia. A similar computation for total exposure over the same period as a result of the GCR background revealed that the change in exposure in equatorial regions as a result of GLE 73 was negligible, while in polar regions the total exposure increased by $\approx 30\%$. The annual exposure of a pilot is typically 3mSv and for the general public, it is 1mSv [21], from this, we can tell that the impact GLE 73 had on human health is small, even in polar regions.

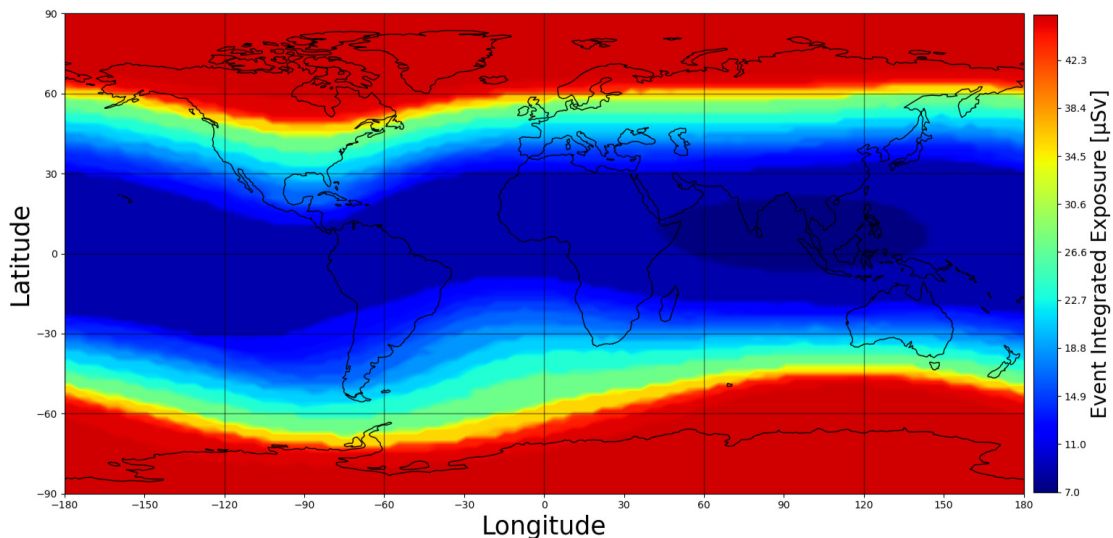


Figure 1: Global event integrated exposure during GLE 73 at FL350.

A comparison between the relative increases in dose and count rate at the south pole NM (SOPO) for two different altitudes is shown in Fig. 2. One can see that there is a very strong relationship between the modelled dose and count rate increases at 35kft, the relationship is less clear at 50kft. We expect higher altitudes to have a greater increase in radiation as a result of less atmospheric shielding in these regions, this is seen in Fig. 2. The particle flux peak for GLE 73 from the derived spectrum, 18:15, is represented in the 50kft plot within Fig. 2, but not in the 35kft

plot. This is due to the spectrum softening over the event leading to the lower energy particles in the latter half of the event not reaching lower altitudes. Note that the general trend for the relative NM count rate increase also decreases over the particle flux peak of GLE 73 as fewer particles reach the surface. The largest increase in radiation dose at 35kft is seen at the start of the GLE when the spectrum is harder meaning higher energy particles are able to penetrate deeper into the atmosphere.

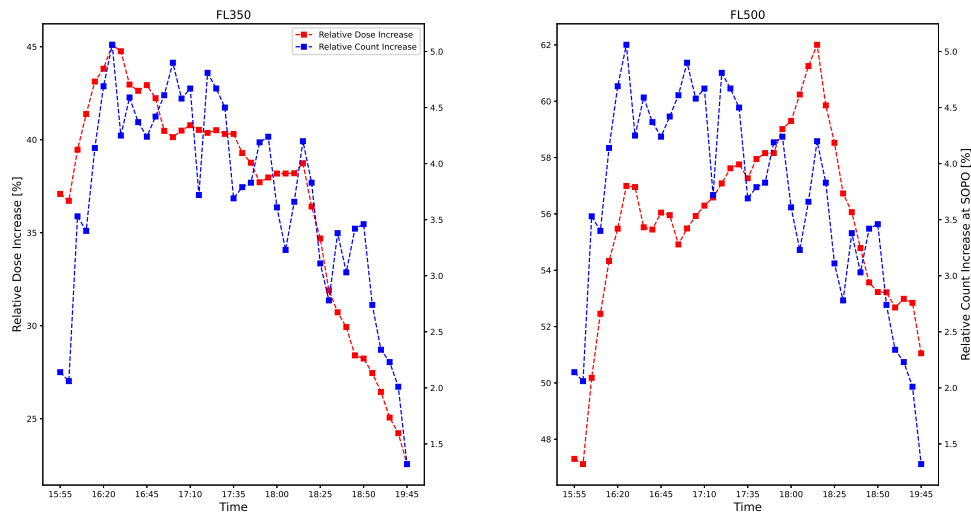


Figure 2: Relative increases in effective dose rate and NM (SOPO) count rate over the duration of GLE 73 at the altitudes of 35kft (left) and 50kft (right).

5. Conclusion

The most recent GLE at the time of writing, GLE 73, has been analysed in past work in order to determine its spectral and angular characteristics; this work expands upon this prior work by investigating the impact GLE 73 had on the radiation dose experienced at aviation altitudes. The results of this investigation show that the space weather impact of GLE 73 was minor with a maximum relative increase in dose above the typical GCR background of $\approx 30\%$ being seen in polar regions, as such this event would provide only a small amount of the average person's or pilot's annual exposure. The impact of GLE 73 on equatorial regions was found to be negligible.

The relative increase in dose computed by the Oulu CRAC:DOMO radiation model was compared to the relative increase in NM count rate at SOPO. At 35kft a clear relationship between the two is seen for GLE 73, this can prove beneficial in the search for a reliable nowcasting tool that uses live NM data to predict radiation at aviation altitudes. Each GLE is different so further investigations of this relationship for other GLEs are needed. At 50kft the increase in radiation dose was greater, but the relationship with NM count rate was less clear, this can be due to the softening of the SEP spectra during the event. More work should be done to investigate the relationship at higher altitudes in the future.

6. Acknowledgements

This study was supported by The Academy of Finland (project 330064 QUASARE and 321882 ESPERA) and benefited from the University of Oulu grant SARPEDON. We acknowledge the neutron monitor database (NMDB) and all colleagues working at the NM stations, with particular thanks to those at SOPO whose data is used within this work. The Finnish Academy of Science and Letters provided additional support to this work via the Vilho, Yrjö and Kalle Väisälä grant.

References

- [1] M. Desai and J. Giacalone, *Large gradual solar energetic particle events*, *Living Reviews in Solar Physics* **13** (2016) 3.
- [2] H. Moraal and K. McCracken, *The time structure of ground level enhancements in solar cycle 23*, *Space Science Reviews* **171** (2012) 85.
- [3] K.-L. Klein and S. Dalla, *Acceleration and propagation of solar energetic particles*, *Space Science Reviews* **212** (2017) 1107.
- [4] D. Cooke, J. Humble, M. Shea, D. Smart, N. Lund, I. Rasmussen et al., *On cosmic-ray cutoff terminology*, *Il Nuovo Cimento C* **14** (1991) 213.
- [5] M. Gerontidou, N. Katzourakis, H. Mavromichalaki, V. Yanke and E. Eroshenko, *World grid of cosmic ray vertical cut-off rigidity for the last decade*, *Advances in Space Research* **67** (2021) 2231.
- [6] S. Poluianov, I. Usoskin, A. Mishev, M. Shea and D. Smart, *Gle and sub-gle redefinition in the light of high-altitude polar neutron monitors*, *Solar Physics* **292** (2017) 176.
- [7] M. Shea and D. Smart, *Space weather and the ground-level solar proton events of the 23rd solar cycle*, *Space Science Reviews* **171** (2012) 161.
- [8] O. Raukunen, R. Vainio, A.J. Tylka, W.F. Dietrich, P. Jiggins, D. Heynderickx et al., *Two solar proton fluence models based on ground level enhancement observations*, *J. Space Weather Space Clim.* **8** (2018) A04.
- [9] S. Koldobskiy, O. Raukunen, R. Vainio, G. Kovaltsov and I. Usoskin, *New reconstruction of event-integrated spectra (spectral fluences) for major solar energetic particle events*, *Astronomy and Astrophysics* **647** (2021) A132.
- [10] A. Mishev, L. Kocharov, S. Koldobskiy, N. Larsen, E. Riihonen, R. Vainio et al., *High-resolution spectral and anisotropy characteristics of solar protons during the gle n°73 on 28 october 2021 derived with neutron-monitor data analysis*, *Solar Physics* **297** (2022) 88.
- [11] A. Mishev and I. Usoskin, *Analysis of the ground level enhancements on 14 july 2000 and on 13 december 2006 using neutron monitor data*, *Solar Physics* **291** (2016) 1225.

- [12] A. Mishev, S. Poluianov and S. Usoskin, *Assessment of spectral and angular characteristics of sub-gle events using the global neutron monitor network*, *Journal of Space Weather and Space Climate* **7** (2017) A28.
- [13] A. Mishev, I. Usoskin, O. Raukunen, M. Paassilta, E. Valtonen, L. Kocharov et al., *First analysis of gle 72 event on 10 september 2017: Spectral and anisotropy characteristics*, *Solar Physics* **293** (2018) 136.
- [14] A. Mishev, S. Koldobskiy, I. Usoskin, L. Kocharov and G. Kovaltsov, *Application of the verified neutron monitor yield function for an extended analysis of the gle # 71 on 17 may 2012*, *Space Weather* **19** (2021) e2020SW002626.
- [15] K. Levenberg, *A method for the solution of certain non-linear problems in least squares*, *Quarterly of Applied Mathematics* **2** (1944) 164.
- [16] D. Marquardt, *An algorithm for least-squares estimation of nonlinear parameters*, *SIAM Journal on Applied Mathematics* **11** (1963) 431.
- [17] A. Mishev and I. Usoskin, *Assessment of the radiation environment at commercial jet-flight altitudes during gle 72 on 10 september 2017 using neutron monitor data*, *Space Weather* **16** (2018) 1921.
- [18] A. Mishev, A. Binios, E. Turunen, A.-P. Leppänen, N. Larsen, E. Tanskanen et al., *Measurements of natural radiation with an mdu liulin type device at ground and in the atmosphere at various conditions in the arctic region*, *Radiation Measurements* **154** (2022) 106757.
- [19] A.L. Mishev, S.A. Koldobskiy, G.A. Kovaltsov, A. Gil and I.G. Usoskin, *Updated neutron-monitor yield function: Bridging between in situ and ground-based cosmic ray measurements*, *Journal of Geophysical Research: Space Physics* **125** (2020) e2019JA027433.
- [20] N. Larsen, A. Mishev and I. Usoskin, *A new open-source geomagnetosphere propagation tool (otso) and its applications*, *Journal of Geophysical Research: Space Physics* **128** (2023) e2022JA031061
[<https://agupubs.onlinelibrary.wiley.com/doi/pdf/10.1029/2022JA031061>].
- [21] L. Bennett, B. Lewis, B. Bennett, M. McCall, M. Bean, L. Doré et al., *A survey of the cosmic radiation exposure of air canada pilots during maximum galactic radiation conditions in 2009*, *Radiation Measurements* **49** (2013) 103.